Iraqi Geological Journal

Journal homepage: https://www.igj-iraq.org

Physico-Chemical, Mineralogical Properties and Valorization of Bentonite Material from Iboughardain Area (North-Eastern Rif, Morocco): Application in Dyes Removal

Yassine Et-Tayea[1], Rachid Cherouaki[1], Ahmed Rachid[1], Hicham Nasri[2], Achraf Harrati[3], Younes Mamouch[1], Jamal Naja[1]

[1] Laboratory Physico-chemistry of Processes and Materials (PCPM), Research Team: Geology of Mining and Energy Resources (GRME), Hassan First University of Settat, Faculty of Sciences and Technology, 26002, Settat, Morocco
[2] Applied Geosciences Laboratory, Geology Department, Mohammed I University, Faculty of Sciences, 60000, Oujda, Morocco
[3] Laboratory of Physical-Chemistry, Materials and Catalysis (LCPMC), Geomaterials and Materials for Energy Team, Hassan II University of Casablanca, Faculty of Sciences Ben M'Sick, Casablanca, Morocco
* **Correspondence**: y.et-tayea@uhp.ac.ma

Received:
4 November 2022

Accepted:
5 March 2023

Published:
31 July 2023

Abstract

This paper focuses on the characterization and valorization of Moroccan bentonite in dye removal. The stratiform Iboughardain deposit is located in Kert basin (Northeast Rif, Morocco), It is accessible via a tarred road connecting Nador-Seghanghan-Dar Kabdani at a distance of approximately 30 km from Nador. Its Lambert coordinates are X = 709.300, Y = 501.000 (topographic sheet Kebdani to 1/100.000). Bentonite outcrops occur as alterations of the lower horizontal layers of trachyandesite tuff and cinerite. This alteration is in contact with greenish Miocene marl. The mineralogy composition of the samples examined indicates the presence of various contents of montmorillonite and associated minerals such as feldspars and quartz. The mineralogy dominated by aluminosilicates is reflected in the chemical composition which shows high contents of SiO_2 and Al_2O_3. The other oxides have moderate proportions. It is Fe_2O_3 (1.90 wt%), K_2O (0.90 wt%), MgO (5.65 wt%), and MnO (0.07 wt%). Geotechnical results show that the sample is very plastic. Importantly, the experimental adsorption results clearly demonstrate that the clay from the Iboughardain region effectively clarifies the dyeing. The removal of methyl orange (CMO = 140 mg/l) was shown to be significant (98%) under activated bentonite compared to doped bentonite (B-TiO_2 20%wt). In addition, the removal of methylene blue staining at a high concentration (CMB = 120 mg/l) was able to reach significant removals of 80 and 99.9% using raw and doped bentonite, respectively.

Keywords: Bentonite clay; Mineralogy; Montmorillonite; Adsorption; Dyes removal; Moroccan Rif

1. Introduction

Most detrital clay minerals are derived from physical or chemical changes in existing rocks (Millot, 1964) and are composed of minerals whose particles are essentially phyllosilicates (Bailey, 1980; Decarreau, 1990). The clay that is the subject of this work is known as "bentonite". It is mainly composed of clay materials formed by the alteration of vitreous igneous rocks such as tuff and volcanic ash (Ross and Shannon, 1926; Wilson, 2007). These clay minerals are associated with minerals typical of igneous rocks (Ross and Shannon, 1926; Grim, 1988; Wilson, 2007). It is characterized by geological formation

DOI: 10.46717/igj.56.2A.6ms-2023-7-15

patterns, mineralogy and chemical composition, swelling and absorption rates, grain size distribution, structural and geotechnical properties (Zheng et al., 2020).

Bentonite proves to be an effective material for removing heavy gasoline ions (Pawar et al., 2016; Maleki et al., 2019). Montmorillonite is considered as the primary mineral in bentonite. It is a 2:1 type of aluminosilicate made up of a central aluminum oxide octahedral, two silicon-oxygen tetrahedra, and interlayer space (Komine and Ogata, 2004). The unit cell subcaste structure contains some cations similar to Cu2+, Mg2+, Na+, and K+. Still, these cations with the unit cell action are fluently exchange with other cations in the result and are largely unstable. (Zhang et al., 2012; Anirudhan and Ramachandran, 2015). Bentonite is therefore cracterized by a high cation exchange capacity. In addition, bentonite present some exceptional physicochemical parcels including a large specific face area, chemical stability, ubiquitous vacuity, high porosity, and low cost (Bhatt et al., 2012; Liu et al., 2016; Yu et al., 2017). Based on these advantages, the capacity of bentonite to adsorb heavy essence ions in wastewater has great exploration possibility. Bentonites are characterized by chemical and mineralogical compositions, ion exchange capacity, adsorption capacity, swelling index, geotechnical, and textural properties (Zheng et al., 2020). The understanding and knowledge of these geotechnical and chemical properties allow defining the most appropriate application of bentonite (Gupta and Kant, 2013). The Iboughardain deposit is part of the Kert basin formed by Neogene volcanic deposits resulting from the alteration of volcanic ash and is a pyroclastic flow with typical transport properties (Ddani et al., 2005).

In addition, in the adsorption process, it is strongly recommended to use supports with a high specific surface area that increases the rejection of adsorbed elements. Clays are one of these supports and among the most suitable materials with a higher specific surface. Thus, clays of the smectite family exhibit such characteristic varies in the range (700 to 840 m2/g) (Hmeid et al., 2021). In previous works, bentonite has been found characterized by a large specific surface area, ranging from 127.62 to 693.04 m2/g, which is due to the presence of intercalated hydrated cations (Ait Hmeid et al., 2021). For this reason, bentonite from this region was a suitable candidate for the current work. The main objective of this work is to define and value smectite clays from the Iboughardain deposit by mineralogical, physicochemical, morphological, and lithological investigations to estimate their treatment and production potential for Application in dyes removal. A representative sample from the deposit will be used to study the adsorption of colorants Methylene Blue and Methylene Orange.

2. Regional Geological Framework

The eastern Moroccan Rif is a structural transition between the Rif orogen, of which it is mostly the outer zones (Intrarif, Mesorif, and Prerif), and the mid-Atlantic front, to which its southern parts belong (Wildi, 1983). diSeveral sedimentary basins formed during the Tortonian-Messinian and Pliocene periods because of their tectonic history (Piqué et al., 1998). The Gourougou complex was created by extensive volcanic activity in conjunction with subduction processes (Maury et al., 2000). The latter is a 15-kilometer-wide stratovolcano surrounded by satellite domes: Tois Fourche, Amjar, Tidiennit, and Beni Bou Ifrour. This massif's structure (Fig. 1b) suggests that the first stage was submerged by explosive volcanic activity. The behavior then grew further airborne and exuberant (Hernandez, 1983; El Bakkali, 1995).

The Beni Bou Ifrour massif is located in the Extra Rif Domain's Mesorif zone, in the original eastern half of the Mesorif zone. This massif is primarily made up of Mesozoic to Neogene sedimentary, volcanic, and granodioriterrocks (Rhazi and Hayashi, 2002). The region's known bentonite deposits are strongly associated with the volcanic formations of the Melilla-Nador and Kert basins and are found in the marine sedimentary succession of these Neogene basins or in "pockets" on the volcanoes' periphery (Hilali and Jeannette, 1981). Geographically, the Iboughardain deposit is part of the Beni Bou Ifrour

massif and is located in the province of Nador (Eastern Moroccan Rif), a commune of Beni Sidel. It is accessible via a tarred road connecting Nador-Seghanghan-Dar Kabdani at a distance of approximately 30 km from Nador. Its Lambert coordinates are X = 709.300, Y = 501.000 (topographic sheet Kebdani to 1/100.000) (Fig. 1a).

This deposit is in the form of irregular lenses of several meters thick intercalated in the Messinian sedimentary sequence near the volcanic devices. They are caused by the partial or complete transformation of pyroclastic products deposited in marine environments to lagoon-lacustrine pyroclastic products. It's a stratiform site located 5 kilometers south of Tidiennit site (Fig. 1a). It is formed by pyroclastic lenses interbedded in Messinian sediments (Ddani et al., 2005).

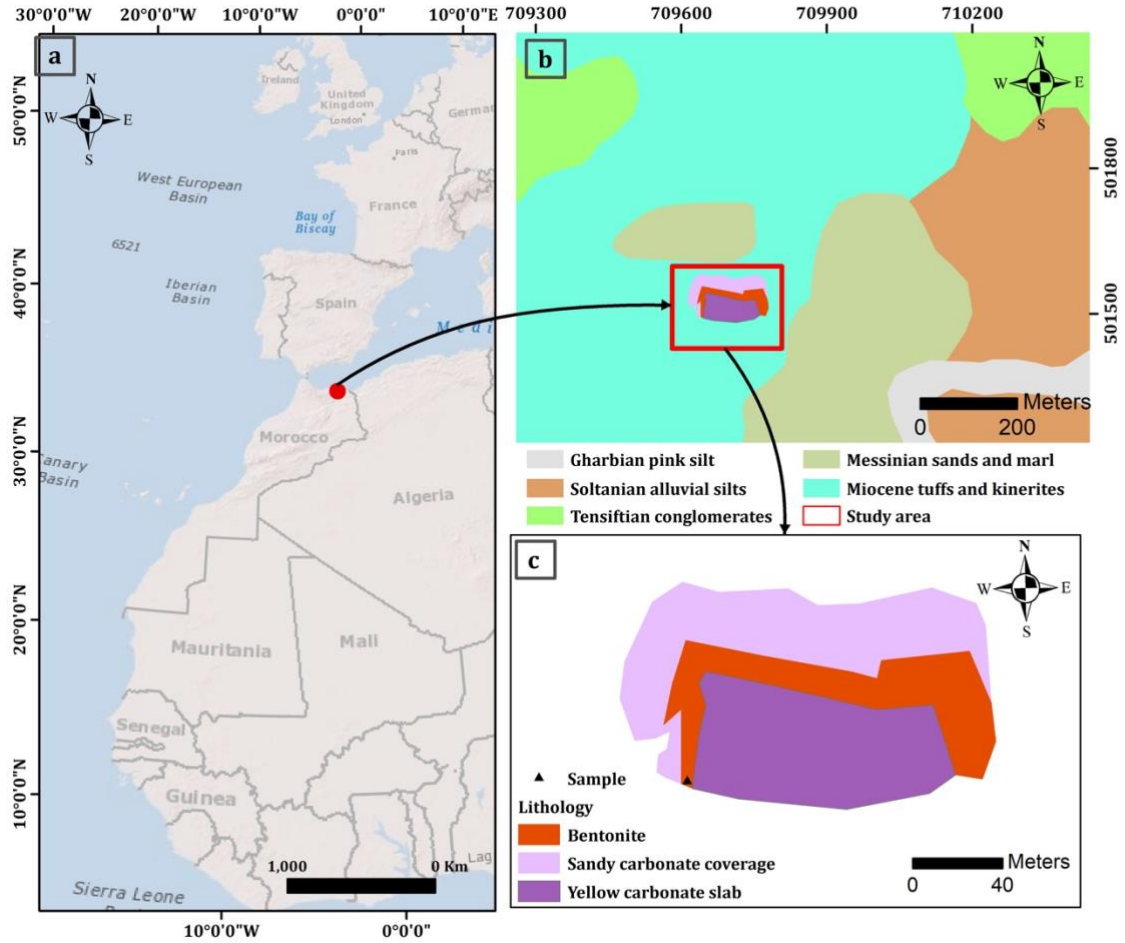

Fig. 1. (a) Index map of the geology and the location of the main bentonite deposits (Mine & géologie, n°14, 1961). (b) A modified geological map extracted from Zghenghen geological map (Ministère de l'Energie et des Mines Direction de la Géologie Editions du Service Géologique du Maroc, Notes et Mémoires N°370 map published in 1996).

3. Materials and Methods

3.1. Materials

The bentonite sample studied was taken from Iboughardain area (Fig. 1b). The sample was initially characterized and then used in the absorption of Colorants (i.e., Methylene blue and methylene orange), in both cases raw and doped with different TiO2 mass percentages.

Methylene blue (MB) is used as a histological stain, and for blue staining of tissue collagen. It is often used as a representative model for medium-sized organic pollutants. It is simple to study the pollution by MB in an aqueous solution since the molecule is characterized by its blue color more or

less intense according to the concentration of the pollutant. Its physico-chemical characteristics are presented in Table 1. The absorption peak is located around 670 nm (Hegazy and Prouzet, 2013). Its structure is presented in Fig. 2.

Table 1. Characteristics of methylene blue.

Colorant	Molar mass (g/mol)	Solubility (g/l) (Water, 20 °C)	pKa	Fusion point (°C)
Colorant	319.86	50	8.28	190

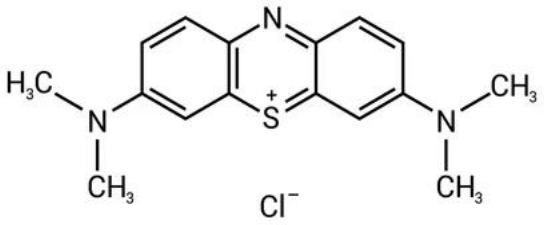

Fig. 2. Molecular structure of methylene blue.

Methylene Orange known as helianthin, was chosen as a simple model of a series of common azo colorants, classified C.I. 13025, and widely used in industry. Its physico-chemical characteristics are displayed in Table 2 and its structure is shown in Fig. 3.

Table 1. Characteristics of the molecular structure of methyl orange.

Colorant	Molar mass (g/mol)	Solubility (g/l) (Water, 20 °C)	pKa	Fusion point (°C)
Methylene Orange	305.35	5.2	3.39	> 300

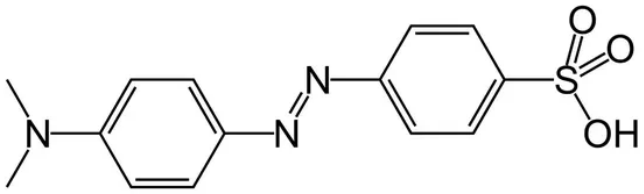

Fig. 3. Molecular structure of methyl orange.

3.2. Geological Survey and Sections of Iboughardain Bentonite

The Iboughardain deposit is part of the Kert basin which is formed by neogene volcano-sedimentary products, resulting from the alteration of volcanic ash and pyroclastic flows which have typical transport characteristics. This alteration occurs at contact with the Miocene greenish marls (Ddani et al., 2005).

The bentonite showings are in the form of two layers; (1) A whitish lower layer of about 5 meters thick overcomes greenish marl, it is covered by cinerites. (2) And an upper layer of about 3.5 meters

thick surmounts on volcanic ash (cinerite) (Fig. 4). These are housed in a subsoil of sandy marl (Asebriy and Cherkaoui, 1995; Ddani et al., 2005), which shows compatibility with the stratigraphic log realized at this deposit.

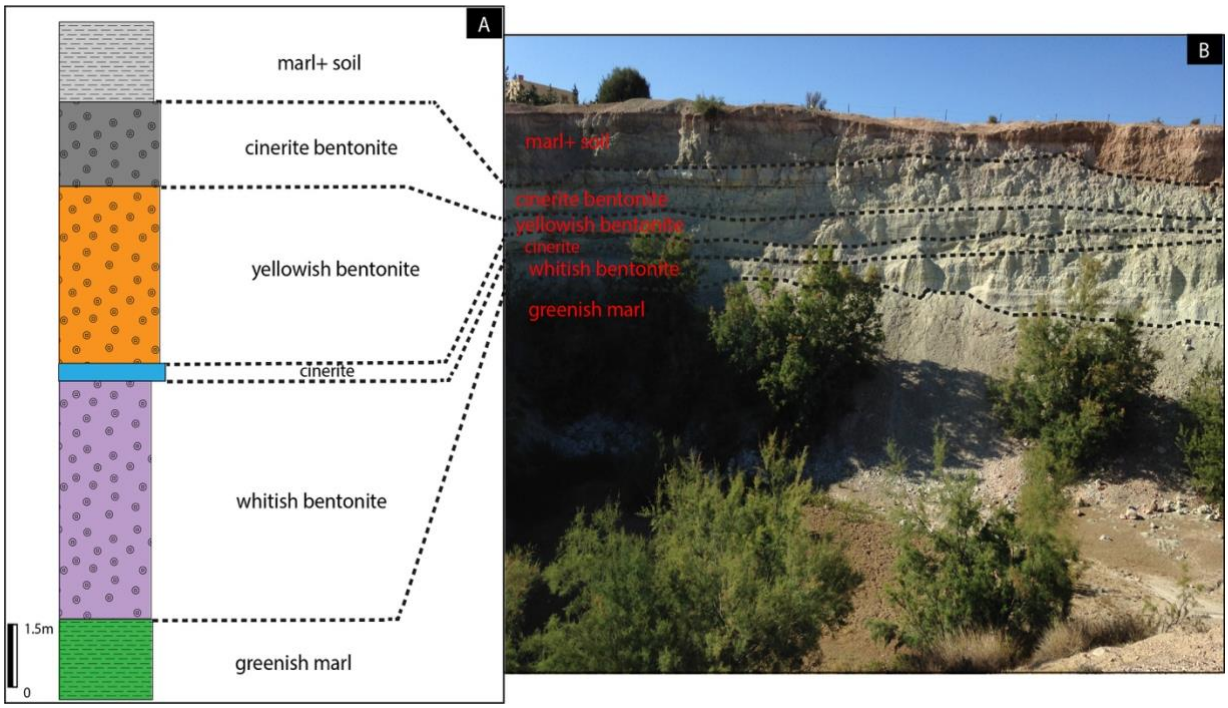

Fig. 4. (A) Synthetic log of Iboughardain deposit. (B) General view of the Iboughardain deposit.

3.3. Mineralogical, Chemical, and Morphological Analysis

Mineralogical analysis was carried out by X-ray diffraction (XRD) using an X'PERT PRO diffractometer using CuKα1 radiation (λ = 1.5418 Å) in RUMINEX, Marrakech, Morocco. Bulk samples were prepared by grinding approximately 1 gram of dry bentonite using a pestle and mortar. Gently push the resulting powder into the sample holder to limit the preferential orientation (Moore and Reynolds, 1998). The XRD pattern was analyzed using the the PDF-2 crystallographic database and X`Pert HighScore Plus software. The chemical analysis was performed at the National Office of Hydrocarbons and Mines (ONHYM) in Rabat, Morocco. Principal component analysis was performed using X-ray fluorescence analysis. The sample powder was mixed well with lithium borate (Li2B4O7), then poured into a troche and pressed into a flat bead shape. The results obtained are presented in mass percentage of the oxide. The sample was heated for 2 h at 1000 °C under oxidizing conditions to obtain ignition loss (LOI). Microstructure analysis was performed by combining an energy dispersive spectroscopy (SEM-EDS) and scanning electron microscope to investigate the morphology, composition, and texture of the bentonite sample. Observations were made at the Regional Center for Analysis and characterization of the Faculty of Science and Technology of Settat in Morocco (CRAC-FSTS) using the Jeol JSM 5600LV scanning electron microscope. The sample has undergone a carbon metallization step in advance to increase the conductivity of the surface so that high-quality images can be taken.

3.4. Physical, Textural, and Geotechnical Analysis

The swelling index of the tested sample was calculated according to the French standard XF P 84703 (Touze-Foltz et al., 2013) at the National Office of Hydrocarbons and Mines (ONHYM) in Rabat-Morocco. To do this, sprinkle 2 g of finely ground bentonite powder (<160 µm) on 80 ml of distilled water in the burette. Then gradually adjust the amount of solution to the 100 ml mark. The swelling index is the volume occupied by 2 g of swollen bentonite after 24 h of hydration and is expressed in ml/g. The Atterberg limits, namely the plasticity limit (PL), the liquid limit (LL), and the plasticity index (PI) have been calculated according to the French standard NFP 94051 (NF, 1993) using the Casagrande method in the Laboratory of Expertise's, Studies and Tests (LEEE), Essaouira (Morocco).

The ability of clay to adsorb cations in solution and its reaction was defined by the relationship between the cation exchange capacity (CEC) and the quantity of methylene blue absorbed by the clay sample. Due to the formation of negative charges at the edges and the homomorphic substitution of tetrahedral and octahedral sheets (Ammann et al., 2005), and because of the the presence of permanent charges, the clay minerals are negatively charged. Cation exchange capacity (CEC) represent the number of monovalent cations that can be exchanged for charge-compensated cations to balance the charge of 100 g of calcined clay (CEC in meq / 100 g of calcined clay).

The cation exchange capacity CEC of bentonite was carried out by using the cobalt hexamine method according to the French standard NF X 31130 (NF, 1999). This mode of operation uses cobalt chloride hexamine. After exchanging the bentonite cation with [Co(NH3)6]3+ ions, the CEC estimate is grounded on the measurement of Co remaining in the solution. The CEC was conducted at the Soil-Water-Plant laboratory, Mohamed V Polytechnic University, Morocco.

4. Results and Discussions

4.1. Mineralogical Composition

The mineralogical composition of the Iboughardain sample investigated shows a combination of clay and non-clay minerals which consists mainly of plagioclase of the anorthite type ($CaAl_2Si_2O_8$; Reference code: 00-041-1486), K-Feldspars ($KAlSi_3O_8$; Reference code: 00-019-0926) and montmorillonite ($Na_{0.3}(Al,Mg)_2Si_4O_{10}(OH)_2.8H_2O$; Reference code: 00-029-1499) as the main crystalline phases along with some amount of quartz (SiO_2; Reference code: 00-046-1045). However, small traces of magnetite (Fe_3O_4; Reference code: 00-019-0629), and muscovite ($KAl_2(Si_3Al)O_{10}(OH,F)_2$; Reference code: 00-006-0263) are also observed (Fig. 5).

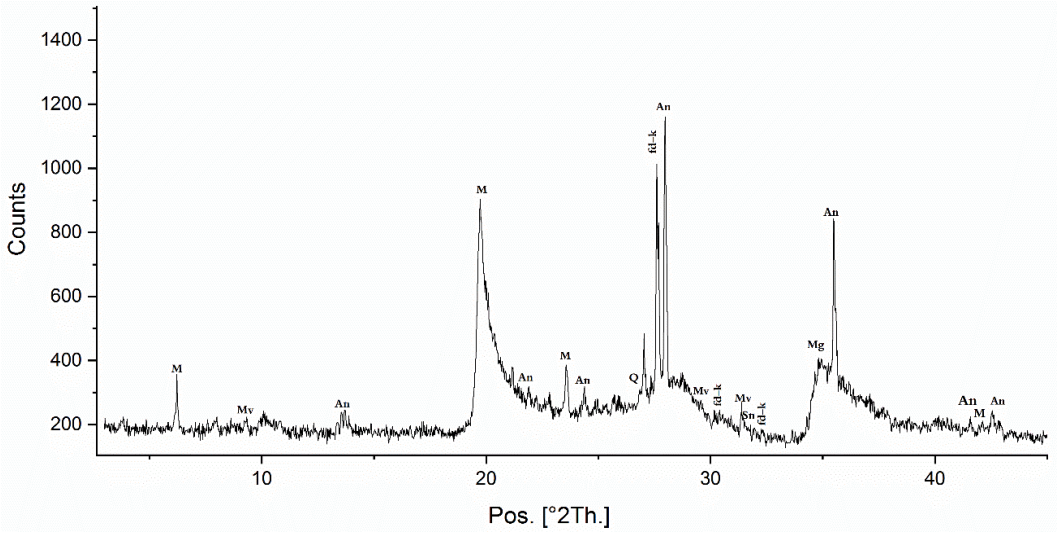

Fig. 5. XRD diffractograms of Iboughardain sample.

4.2. Chemical Composition

The chemical composition is mainly composed of SiO_2 (> 60 wt%) and Al2O3 (> 17 wt%). Iron oxide (Fe_2O_3) values designate that iron cations are present in the smectite interlayer in the absence of minerals such as hematite. Sodium oxide (Na_2O) and calcium oxide (CaO) are present in small amounts (0.80-3.07 wt%).The relative content of MgO (5.65 wt%) is probably originated from montmorillonite clay mineral (El Miz et al., 2017). This corresponds to the presence of montmorillonite and plagioclase (Table 3). The presence of feldspar justified the presence of potassium oxide (K_2O). The values of SiO_2 show that bentonite results from the alteration of acidic volcanic products (trachyte or rhyolites) (Ddani et al., 2005).

Table 2. Chemical composition of the studied samples by weight (wt. %).

Samples	**SiO_2**	**Al_2O_3**	**Fe_2O_3**	**TiO_2**	**CaO**	**MgO**	**Na_2O**	**K_2O**	**MnO**	**P_2O_5**	**LOI**[1]
Ib	60.40	17.69	1.90	0.18	0.80	5.65	3.07	0.90	0.07	0.06	7.58

[1] Loss on ignition at 1000 °C for 2 h.

4.3. Scanning electron microscope observations

The SEM images of the bentonite sample studied show a global aspect of the material whose compact structure can be marked, spherical grains (approximatively of 4-40 µm-sized particles according to SEM scale) show the presence of feldspars. The impurities above these grains with a spongy appearance are alteration products of montmorillonite (Fig. 6).

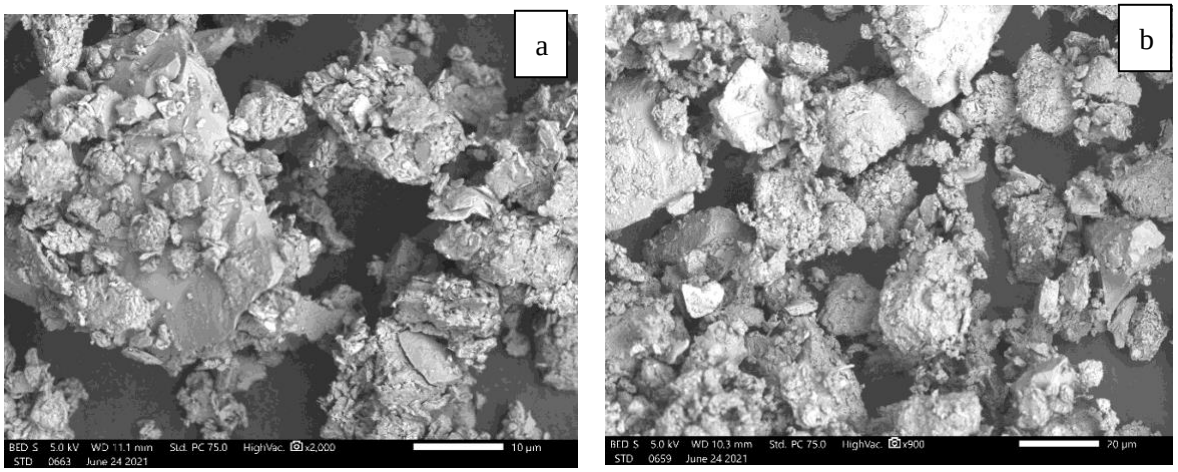

Fig. 6. SEM images of raw sample (a) 10 µm (b) 20 µm.

4.4. Technological Tests

4.4.1. Swelling index

The values of the swelling index for the sample mentioned in Table 4 is 11 ml/2g. After activation with 3 wt% of Na_2CO_3 for 30 minutes of agitation, the swell index increased by 56%. The swell index values are considered high which allows for determining the application fields of bentonite, as swell index tests has been used by the industry as a pre-screening method for qualitatively assessing the quality of bentonites (Waanders et al., 2015).

Table 3. Swelling index of the sample.

Sample	**Natural condition**	**After activation**
	Swell index (ml/2g)	**Swell index (ml/2g)**
Ib	11	25

4.4.2. Atterberg limits

The liquid limit of the sample is 101%, the plastic limit is 67% and the resulting plasticity index is 34% (Table 5), Which means that the sample is extremely plastic (Casagrande, 1948; Holtz et al., 1981) and it is comparable with calcic bentonites (Inglethorpe et al., 1993; Ddani et al., 2005).

Table 4. Atterberg limits of the sample.

	Ib
Atterberg Limits	
LL (%)	101
PL (%)	67
PI (%)	34

4.4.3. Cation exchange capacity

The cation exchange capacity (CEC) of the sample studied is 64.7 meq/100g. This calculated value is lower than the CEC of smectite clay minerals. However, it is higher than kaolinite, illite, and chlorite CEC (Table 6). This is due to the presence of montmorillonite associated with other non-clay minerals (Feldspar, carbonates, etc.).

Table 5. CEC of the sample studied (Ib sample) and some clay minerals (Inoue and Velde, 1995; Morel, 1996; Santamarina et al., 2002; Valencia, 2008).

	Ib sample	**Smectite**	**Illite**	**Kaolinite**	**Chlorite**	**Vermiculite**
CEC (meq/100g)	64.7	80-150	10-40	3-15	10-40	100-150

4.5. Treatment of Colorants with Raw Bentonite

Fig. 7 shows the evolution of colorant abatement as a function of time. It is concluded that the abatement rate of methyl orange does not exceed 13% under the reaction conditions, while it was 100% for methylene blue after 50 min of contact time.

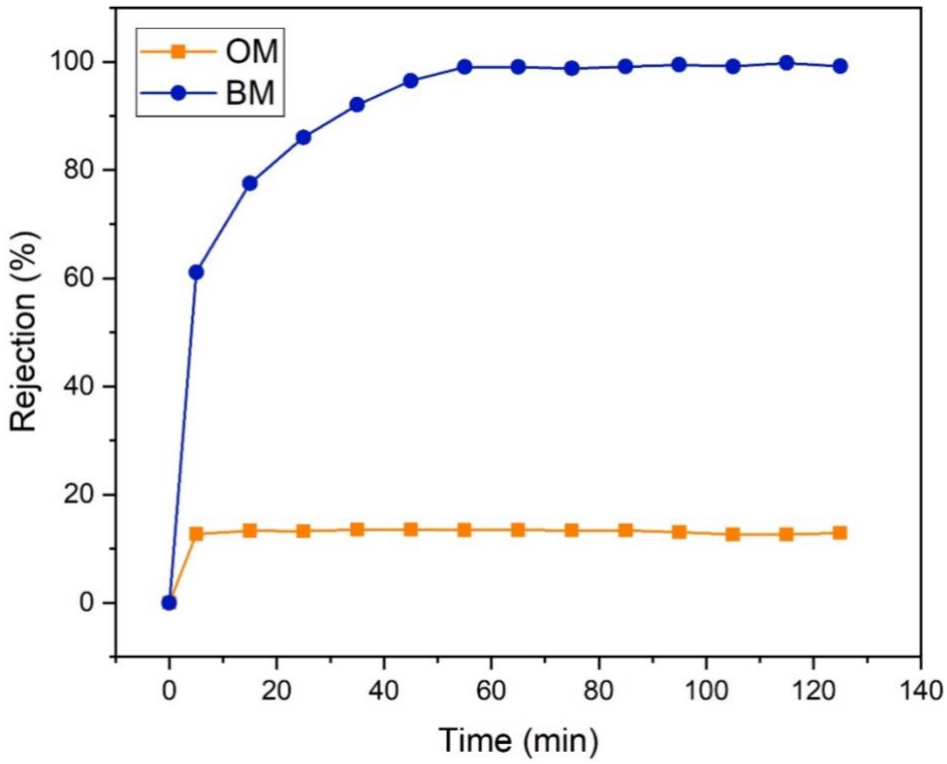

Fig. 6. Abatement of methyl orange (CMO = 40 mg/l) and methylene blue (CMB = 80 mg/l) by raw bentonite.

The clay particles carry a negative structural charge (Dakkach et al., 2012). Alkaline conditions (between pH = 8.5 and 10.0) (Hassine, 2006) increase the action of attraction with methylene blue (cationic colorant) and increase the repulsive action with methyl orange. Therefore, the mechanism of adsorption or desorption is due to Van der Waals forces and ionic forces.

4.6. Treatment of Colorants with Doped Bentonite

To enlarge the effect of some parameters, such as the doping rate, the activation process, and the photon flux, each colorant is treated separately.

4.6.1. Methylene Blue

The evolution of methylene blue abatement as a function of time (Fig. 8) shows that raw or doped bentonite gives similar results in terms of final discoloration, which vary between 90% and 99.9%. Nevertheless, the initial rates of adsorption and/or degradation are higher for raw or doped bentonite at 5%. Whereas they are lower for samples doped at higher rates. This could be explained by the occupation

of the direct adsorption sites by the added TiO_2. Thus, it could be a logical succession of the process which starts first with adsorption and is followed by degradation.

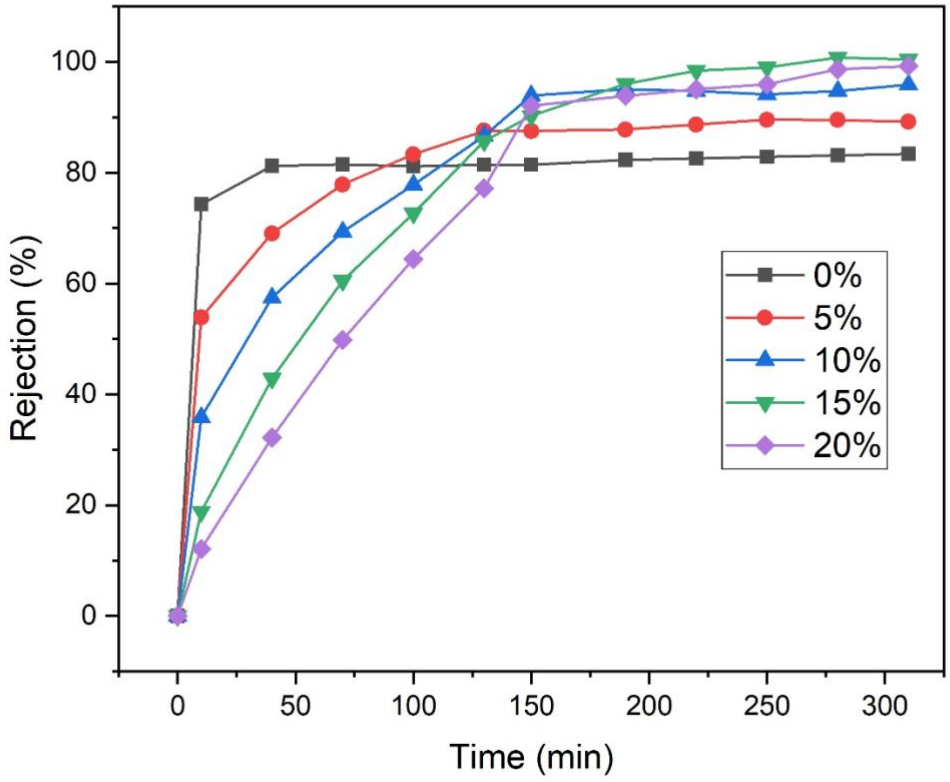

Fig. 7. Evolution of the methylene blue abatement rate (CMB = 120 mg/l) at different TiO_2 rates.

With doped bentonite, the curves show that the discoloration (Fig. 9.) of methylene blue could start first with adsorption followed by degradation by the photocatalyst.

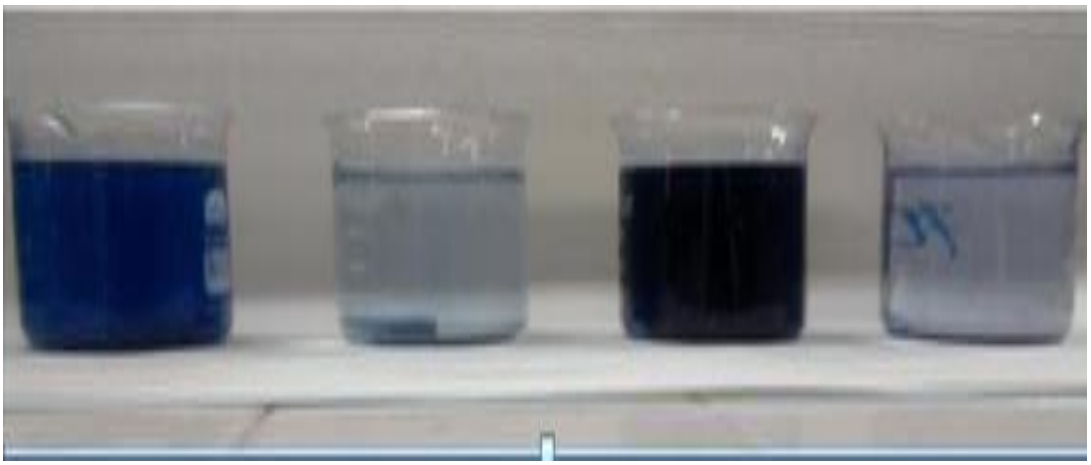

Fig. 8. Comparison between treated and untreated methylene blue.

In Table 7, the initial rates and abatements of methylene blue as a function of doping rate have been grouped. The best removal rate is due to the raw bentonite and as the doping rate increases the initial rate decreases but the rate of color removal increases as the doping rate increases.

Table 6. Initial speeds and final abatement rates.

Bentonite	**Initial speed (mg/l.min)**	**Abatement (%)**
B-TiO_2 (0%)	6.33	80
B-TiO_2 (20%)	1.524	100

4.6.2. Methylene Blue

The variation in the amount adsorbed in methyl orange by raw and doped bentonite is shown in (Fig. 10). It is noted that doped bentonite shows almost the same variation as raw bentonite. The doping has almost no effect on the amount adsorbed.

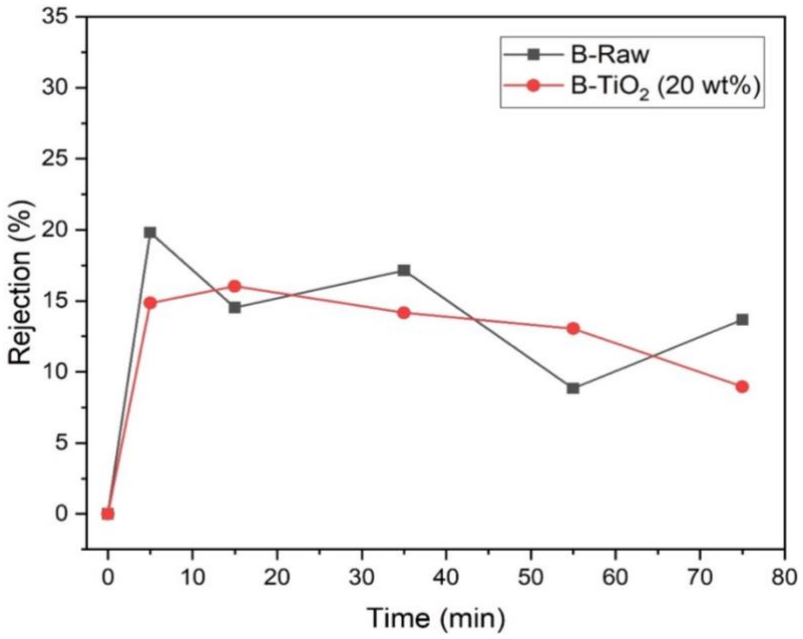

Fig. 9. Variation in the amount of methyl orange adsorbed (CMO = 40 mg/l).

Also, a fluctuation of the quantity adsorbed in methyl orange is observed, which could be explained by an alternation of the adsorption/desorption cycle. To remedy this problem, an acid activation was tested, by adding 4 ml/l of HCl. Indeed, activation is a complex process that involves a series of chemical reactions, and it increases the specific surface. The latter increases from 40-60 m2/g to almost 200 m2/g for dry clay (Leodopoulos et al., 2012). The variation of the quantity adsorbed in methyl orange by the doped bentonite (B-TiO_2%) not activated and the raw bentonite activated by the addition of HCl, is illustrated in the following (Fig. 11) for a concentration of 140 mg/l of methyl orange. The acid activation of bentonite (B-TiO_2 (0 wt%), B-TiO_2 (20 wt%)) allowed a significant increase in the amount of adsorbed colorant, reaching an abatement rate of nearly 98%.

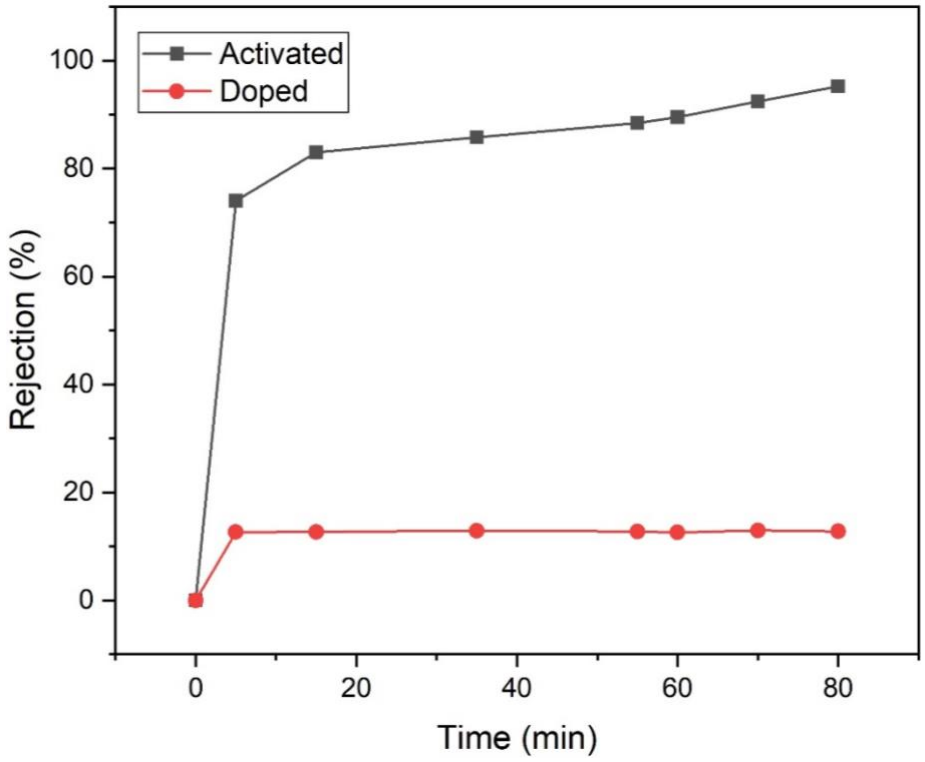

Fig. 10. Evolution % of methyl orange removal on doped (Red curve) and activated bentonite (Black curve).

5. Conclusions

This work is part of the sustainable development and valorization of bentonite-type clay as a natural resource suitable for the abatement of polluting molecules. The preparation of adsorbents with high adsorption capacity is generally divided into two categories:

- Carbonaceous adsorbents consist mainly of carbon, hydrogen, oxygen, and possibly nitrogen.
- The mineral adsorbents are generally materials that have active functional sites, which confer them the properties of adsorption.

Due to of this, alternative technologies and adsorbents have been studied for the treatment of dyes in recent years. Many of these adsorbents are available in large quantities as natural materials, and with low prices, including clay, are phyllosilicates consisting of two tetrahedral layers interspersed by an octahedral layer. Mineralogically this family consists of several species such as montmorillonite, beidellite, hectorite, and saponite. The high charge of these clays is mainly due to isomorphic substitutions. This charge is thus negative and little dependent on the pH. It is compensated by the exchangeable cations (Na^+, Mg^{2+}, Ca^{2+}...), placed between the sheets. The mineralogy composition of the samples studied indicates the presence of various contents of montmorillonite and associated minerals such as feldspars and quartz. The mineralogy dominated by aluminosilicates is reflected in the chemical composition which shows high contents of SiO2 and Al2O3. The other oxides have moderate proportions. It is Fe_2O_3 (1.90 wt%), K_2O (0.90 wt%), MgO (5.65 wt%), and MnO (0.07 wt%). Geotechnical results show that the sample is very plastic.

The experimental adsorption results clearly demonstrate that the clay from the Iboughardain region effectively clarifies the dyeing. The removal of methyl orange (CMO = 140 mg/l) was shown to be significant (98%) under activated bentonite compared to doped bentonite (B-TiO_2 20%wt). In addition, the removal of methylene blue staining at a high concentration (CMB = 120 mg/l) was able to reach significant removals of 80 and 99.9% using raw and doped bentonite, respectively. Bentonite has a

lamellar structure favorable to the incorporation in the interlamellar space of organic molecules, cations, or anions, they can fix many molecules through hydrogen bonds.

References

Ait Hmeid, H., Akodad, M., Baghour, M., Moumen, A., Skalli, A., Azizi, G., Gueddari, H., Maach, M., Aalaoul, M., Anjjar, A., 2021. Valorization of Moroccan Bentonite Deposits:"Purification and Treatment of Margin by the Adsorption Process. Molecules, 26, 5528.

Ammann, L., Bergaya, F., Lagaly, G., 2005. Determination of the cation exchange capacity of clays with copper complexes revisited. Clay Minerals, 40, 441–453.

Anirudhan, T.S., Ramachandran, M., 2015. Adsorptive removal of basic dyes from aqueous solutions by surfactant modified bentonite clay (organoclay): kinetic and competitive adsorption isotherm. Process Safety and Environmental Protection, 95, 215–225.

Asebriy, L., Cherkaoui, T.E., 1995. Tectonique cassante et sismotectonique dans le Rif et son avant-pays (Maroc). Africa Geosciences Review 2, 181–188.

Bailey, S.W., 1980. Summary of recommendations of AIPEA nomenclature committee. Clays and Clay Minerals, 28, 73–78.

Bhatt, A.S., Sakaria, P.L., Vasudevan, M., Pawar, R.R., Sudheesh, N., Bajaj, H.C., Mody, H.M., 2012. Adsorption of an anionic dye from aqueous medium by organoclays: equilibrium modeling, kinetic and thermodynamic exploration. RSC Advances, 2, 8663–8671.

Casagrande, A., 1948. Plasticity chart for the classification of cohesive soils. Transacfions of the American Society of Civil Engineering, 113, 901–930.

Dakkach, M., Atlamsani, A., Sebti, S., 2012. Le phosphate naturel modifié au vanadium: un nouveau catalyseur pour l'oxydation des cycloalcanones et des α-cétols en présence de l'oxygène moléculaire. Comptes Rendus Chimie, 15, 482–492.

Ddani, M., Meunier, A., Zahraoui, M., Beaufort, D., El Wartiti, M., Fontaine, C., Boukili, B., El Mahi, B., 2005. Clay mineralogy and chemical composition of bentonites from the Gourougou volcanic massif (northeast Morocco). Clays and Clay Minerals, 53, 250–267.

Decarreau, A., 1990. Matériaux argileux: Structure, propriétés et applications. Société française de Minéralogie et de Cristallographie et Groupe Français ….

El Bakkali, S., 1995. Volcanologie et magmatologie du système du Gourougou (Rif oriental, Maroc).

El Miz, M., Akichoh, H., Berraaouan, D., Salhi, S., & Tahani, A. (2017). Chemical and physical characterization of moroccan bentonite taken from nador (north of Morocco). American Journal of Chemistry, 7(4), 105-112.

Grim, R.E., 1988. The history of the development of clay mineralogy. Clays and Clay Minerals, 36, 97–101.

Gupta, A.R., Kant, V., 2013. Research article synthesis, characterization and biomedical applications of nanoparticles, Vijayta Gupta Department of Chemistry, University of Jammu, Jammu-180006, India. Science International 1.

Hassine, H. Ben, 2006. Nature minéralogique et rôle nutritionnel des argiles de sols céréaliers en région subhumide à semi-aride (Tunisie). Comptes Rendus Geoscience, 338, 329–340.

Hegazy, A., Prouzet, E., 2013. Effect of physical chemistry parameters in photocatalytic properties of TiO2 nanocrystals. Comptes Rendus Chimie, 16, 651–659.

Hernandez, J., 1983. Le volcanisme miocène du Rif oriental(Maroc): géologie, pétrologie et minéralogie d'une province shoshonitique.

Hilali, E.A., Jeannette, A., 1981. Bentonites. Mines, Géologie et Énergie, 102–137.

Hmeid, H.A., Akodad, M., Aalaoul, M., Baghour, M., Moumen, A., Skalli, A., Anjjar, A., Conti, P., Sfalanga, A., Khyabani, F.R., 2021. Clay mineralogy, chemical and geotechnical characterization of bentonite from Beni Bou Ifrour Massif (the Eastern Rif, Morocco). Geological Society, London, Special Publications 502, 31–44.

Holtz, R.D., Kovacs, W.D., Sheahan, T.C., 1981. An introduction to geotechnical engineering. Prentice-Hall Englewood Cliffs.

Inglethorpe, S.D.J., Morgan, D.J., Highley, D.E., Bloodworth, A.J., 1993. Industrial Minerals laboratory manual: bentonite. British Geological Survey, Mineralogy and Petrology Group.

Inoue, A., Velde, B., 1995. Origin and mineralogy of clays.

Komine, H., Ogata, N., 2004. Predicting swelling characteristics of bentonites. Journal of Geotechnical and Geoenvironmental Engineering, 130, 818–829.

Leodopoulos, C., Doulia, D., Gimouhopoulos, K., Triantis, T.M., 2012. Single and simultaneous adsorption of methyl orange and humic acid onto bentonite. Applied Clay Science, 70, 84–90.

Liu, S., Li, J., Yang, Y., Wang, J., Ding, H., 2016. Influence of environmental factors on the phosphorus adsorption of lanthanum-modified bentonite in eutrophic water and sediment. Environmental Science and Pollution Research, 23, 2487–2494.

Maleki, A., Hajizadeh, Z., Sharifi, V., Emdadi, Z., 2019. A green, porous and eco-friendly magnetic geopolymer adsorbent for heavy metals removal from aqueous solutions. Journal of Cleaner Production, 215, 1233–1245.

Maury, R.C., Fourcade, S., Coulon, C., Bellon, H., Coutelle, A., Ouabadi, A., Semroud, B., Megartsi, M., Cotten, J., Belanteur, O., 2000. Post-collisional Neogene magmatism of the Mediterranean Maghreb margin: a consequence of slab breakoff. Comptes Rendus de l'Académie Des Sciences-Series IIA-Earth and Planetary Science, 331, 159–173.

Millot, G., 1964. Géologie des argiles: altérations, sédimentologie, géochimie. Masson,.

Morel, R., 1996. Les sols cultivés. Technique & documentation-Lavoisier.

NF, P., 1993. 94-051, 1993. Détermination des limites d'Atterberg—Limite de liquidité à la coupelle-Limite de plasticité au rouleau. Association Française de Normalisation (AFNOR).

Pawar, R.R., Gupta, P., Bajaj, H.C., Lee, S.-M., 2016. Al-intercalated acid activated bentonite beads for the removal of aqueous phosphate. Science of The Total Environment, 572, 1222–1230.

Piqué, A., Brahim, L.A., Maury, R.C., Bellon, H., Semroud, B., 1998. Le poinçon maghrébin: contraintes structurales et géochimiques. Comptes Rendus de l'Académie Des Sciences-Series IIA-Earth and Planetary Science, 326, 575–581.

Rhazi, M.E.L., Hayashi, K., 2002. Mineralogy, geochemistry, and age constraints on the Beni Bou Ifrour skarn type magnetite deposit, northeastern Morocco. Resource Geology, 52, 25–39.

Ross, C.S., Shannon, E. V, 1926. The minerals of bentonite and related clays and their physical properties 1. Journal of the American Ceramic Society, 9, 77–96.

Santamarina, J.C., Klein, K.A., Wang, Y.-H., Prencke, E., 2002. Specific surface: determination and relevance. Canadian Geotechnical Journal, 39, 233–241.

Touze-Foltz, N., Bloquet, C., Barral, C., Oberti, O., Chappe, J., 2013. Évaluation de la performance d'un géosynthétique bentonitique en couverture d'installation de stockage de déchets. 9èmes Rencontres Géosynthétiques. 7p.

Valencia, F., 2008. Caractérisation des particules fines d'un matériau granulaire de fondation par l'essai au bleu de méthylène.

Waanders, F.B., Ungerer, E., Fosso-Kankeu, E., 2015. Correlation between swelling index of bentonite clay and the strength of pellets. 7th International Conference on Latest Trends in Engineering and Technology (ICLTET'2015). 24–27.

Wildi, W., 1983. La chaîne tello-rifaine (Algérie, Maroc, Tunisie): structure, stratigraphie et évolution du Trias au Miocène. Revue de Géographie Physique et de Géologie Dynamique, 24, 201–297.

Wilson, I., 2007. Applied clay mineralogy. occurrences, processing and application of kaolins, bentonite, palygorskite-sepiolite, and common clays. Haydn H. Murray. Developments in Clay Science, volume 2, Elsevier Science, Amsterdam, 2007.

Yu, T., Liang, S., Shang, X., 2017. Kinetic and thermodynamic study of Am (III) sorption on Na-bentonite: Comparison of linear and non-linear methods.

Zhang, Y., Zhao, Y., Zhu, Y., Wu, H., Wang, H., Lu, W., 2012. Adsorption of mixed cationic-nonionic surfactant and its effect on bentonite structure. Journal of Environmental Sciences, 24, 1525–1532.

Zheng, L., Xu, H., Rutqvist, J., Reagan, M., Birkholzer, J., Villar, M.V., Fernández, A.M., 2020. The hydration of bentonite buffer material revealed by modeling analysis of a long-term in situ test. Applied Clay Science 185, 105360.